

PREPRINT of the paper published in:

*Energy & Fuels*, 2006, V.20, Iss.2, pp.682-687.

## **Thermally Responsive Properties of Asphaltene Dispersions**

Igor N. Evdokimov,\* and Nikolaj Yu. Eliseev

*Department of Physics, Gubkin Russian State University of Oil and Gas, Leninsky Prospekt, 65,*

*Moscow B-296, GSP-1, 119991, Russia*

---

\* Corresponding author. *E-mail:* [physexp@gubkin.ru](mailto:physexp@gubkin.ru) , *URL:* <http://eee.gubkin.ru>

### **Abstract**

Mass of deposits at steel surfaces and dynamic viscosity were measured at 10-45°C in model oils (toluene + vacuum residua) with 12.3 g/L asphaltenes. The observed step-like changes of measured parameters at ~27°C were interpreted as indicative of a first-order phase transition to reduced particle volumes in asphaltene colloids. By a number of specific features this transition resembles well-known phenomena at the lower critical solution temperature (LCST) in thermally responsive microgel dispersions of block copolymers. The microgel/LCST analogy is further supported by literature data on the structure of basic asphaltene nanoaggregates. In particular, a comparative asphaltene – microgel discussion shows that the role of hydrogen bonding in primary asphaltene aggregation may be underestimated.

*Keywords:* Asphaltenes; Dispersion; Petroleum; Deposits; Viscosity; Phase behavior;

## 1. Introduction

A typical petroleum fluid contains millions of different molecules and is a hybrid of a solution and a colloidal dispersion. Hence, understanding its phase behavior still remains a challenge even after decades of scientific investigation. The significant portion of colloidal particles is formed by self-associating asphaltenes,<sup>1</sup> which are sometimes referred to as the most enigmatic component of crude oil.<sup>2,3</sup> Asphaltenes have enormous impact in the production, transportation, and refining of crude oil and, thus, property and phase behavior measurements for asphaltenes and asphaltene-bearing media are of extreme interest for many technological and economic applications. Unfortunately, the progress in understanding a behavior of asphaltenes in petroleum has been impeded by several persistent “myths”, which have been properly investigated only recently.

E. g., for long time a commonly accepted view in petroleum science has been that asphaltenes molecules start to aggregate into colloidal “micelles” (sterically stabilized by resins) only at concentrations above a “CMC” of about several grams per litre.<sup>2-6</sup> However, in our 2002 publication<sup>7</sup> we have presented experimental data on optical absorptivity which have shown that aggregation of asphaltenes in toluene solutions is significant already at concentrations as low as 1-2 mg/l. Aggregation proceeds in a reproducible multi-step manner with increasing net asphaltene content both in solutions of solid asphaltenes and in solutions of multi-component crude oils or vacuum residia. Hence, apparently, the role of resins in the initial stages of asphaltene aggregation is not crucial. These data have been further supported by a series of our experiments with highly diluted toluene solutions of oils and of solid asphaltenes, employing techniques of UV-Vis spectroscopy,<sup>4,5</sup> viscometry,<sup>5,8</sup> NMR relaxometry,<sup>5</sup> static light scattering<sup>8</sup> and refractometry.<sup>9</sup> On the basis of this experimental evidence, a scenario of asphaltene phase behavior in petroleum-based fluids/solutions was summarized as follows. Asphaltene “unimers” (nomenclature according to Ref. 10 – cf. Section 4.1) are predominant species only at extremely low concentrations, not exceeding ~1 ppm. At concentrations from ~2-5 to ~90-120 mg/l asphaltenes

aggregate into oligomers of increasing complexity. At asphaltene concentrations of about 100-120 mg/l fluids/solutions become inhomogeneous and start to demix into an asphaltene-rich phase and a hydrocarbon-rich phase. However, no macroscopic phase separation follows, owing to the strongly non-equilibrium character of an asphaltene-rich phase (which may be described as a supersaturated or as a supercooled asphaltene solution). Hence, the emerging local regions of this phase quickly relax not by coalescence into a continuous bulk phase, but by a process of exothermic “nanocondensation” - formation of a nanocolloid system of self-stabilized asphaltene nanoparticles, weakly interacting with each other as compared to asphaltene unimers/oligomers. To distinguish asphaltene nanoparticles with a core-corona structure from frequently cited “micelles”, we have introduced<sup>11,12</sup> the term “molecular nanocluster” (MNC). At still higher concentrations, including those typical for heavy crudes and bitumen, asphaltene MNCs further aggregate (by weak physical interactions) into colloidal species of conventional dimensions. More recently, independent conformations of multi-step aggregation at low asphaltene concentrations have been obtained by several research groups (cf. discussion in Refs. 2,3). A conclusion that a liquid-liquid phase separation (demixing) is involved in shaping the properties of asphaltene colloids also becomes supported by some authors.<sup>13</sup>

Other commonly accepted “myths” in petroleum science have been that at asphaltene concentrations, typical for natural petroleum systems: 1) the structure of asphaltene dispersion is fairly insensitive to small variations of ambient conditions; 2) the state of asphaltenes is thermodynamically controlled. Hence, usually it is implicitly assumed that far from obvious critical/transition points the properties of asphaltene colloids are slowly varying smooth functions of external conditions, e.g. of temperature. Consequently, in a lot of conventional experiments temperature dependencies are investigated with fairly large intervals between consecutive data points, e.g. 15-40°C,<sup>14</sup> 10-20°C.<sup>15</sup> Over the past several years we have conducted a series of rheological experiments with “unconventionally” small temperature increments of 1-2°C.<sup>12,16,17</sup> Unexpectedly, we have observed reproducible non-monotonous temperature dependencies of some rheological parameters at temperatures of 10-50°C, i.e.

at the temperature range of importance for some reservoir fluid applications. These results were interpreted as an evidence of noticeable structural transformations in asphaltene colloids, induced by comparatively small temperature variations close to 26-28°C. The new states of asphaltenes may become long-lived metastable (transient) ones at lower temperatures due to a strong kinetic control of thermally-induced transformations of asphaltenes. Whatever the explanation, these experiments have shown that the observed current properties of an asphaltene-containing fluid may strongly depend on its thermal history.

In the present communication we report the results of new experiments in support of thermally responsive states of asphaltene dispersions. Some preliminary data have been reported at the 2004 International Conference on Heavy Organic Depositions (HOD 2004), Los Cabos, Mexico.<sup>18</sup>

## 2. Experimental

**2.1. Samples.** Experiments have been carried out with asphaltene-rich model oil (asphaltene concentration 12.3 g/l). The light hydrocarbon fractions were represented by toluene, the heavy oil fractions - a vacuum residue from Western Siberian crudes (density at 20°C - 979 kg/m<sup>3</sup> ; pour point - 18°C; boiling point - 342°C; asphaltenes - 10.9 wt. % ). The components were mixed at room temperature 1 month before the experiments and were stored at RT (18-20°C) in a dark glass vessel, in air.

**2.2 Apparatus and procedure.** Measurements of heavy organic deposition were performed at metal substrates – two 1 mm thick steel plates with a total surface area of 256.1 cm<sup>2</sup>. Deposition studies were conducted in a temperature controlled ( $\pm 0.1^\circ\text{C}$ ) glass cell with steel substrates vertically immersed into the model oil, to minimize sedimentation effects. The mass of deposits was determined with an

analytical balance (100 g capacity, 0.1 mg precision). Oil viscosities were measured in a temperature controlled Hoppler-type viscometer.

Between deposition/viscosity experiments, the model oil was stored at RT (18-20°C). Each individual experiment commenced with pre-treating the entire quantity of the model oil at the required measurement temperature for 15-20 minutes. Afterwards several ml of the liquid were transferred either to the deposition cell or to the viscometer. A standard deposition time was 20 minutes (cf. the next Section). Steel samples covered with deposits were dried in warm air and weighted. Before a new experiment the samples were washed in toluene, wiped with a cotton cloth and dried in warm air. This procedure restored the mass of steel plates to within 1 mg of its initial value.

It should be noted, that we had no strict scenario for choosing the individual measurement temperatures (i.e. no prescribed “descending order” or “ascending order”). To improve statistics, each next temperature was set virtually at random in the range of 10-45°C. Hence, in continuing experiments, the state of our model oil acquired more and more complicated thermal history.

### 3. Results

**3.1. Deposition experiments.** Kinetics of deposition has been studied at 20°C. The measured time dependencies resembled those characteristic for multilayer adsorption of complex molecules/polymers.<sup>19</sup> In particular, for adsorption times below 2-3 min, a “rapid” initial adsorption was observed, while at longer times the deposited mass increased very slowly. In a first approximation, adsorption kinetics is often described as a first-order process,<sup>20</sup> which implies a simple dependence for a mass of deposits:

$$M = M_e [ 1 - \exp(-bt) ] \dots\dots\dots(1)$$

where  $b$  is an deposition rate constant,  $M_e$  is an equilibrium mass of deposits. The best fit of eq. (1) to our experimental data was obtained with  $b = 6.4 \text{ min}^{-1}$ . For practical reasons, the standard deposition time of 20 min. was used in further experiments.

The results of a series of deposition vs. temperature experiments are shown in Figure 1. Filled symbols denote the data set for “low temperature equilibrium” (LTE) state of the model oil, which in its thermal history never has been heated above a transition temperature of  $T \approx 27^\circ\text{C}$  (cf. Introduction). The evident property of the LTE state is a slow increase in the mass of deposits  $M$  with increasing  $T$  up to  $\sim 17^\circ\text{C}$ . Apparently, this temperature also has some special significance, as above  $17^\circ\text{C}$   $M$  levels off and shows a tendency to decrease. Finally, in the vicinity of a transition temperature noticeable fluctuations of the deposited mass are observed.

Open symbols in Figure 1 denote the data for the model oil with thermal histories including a structural transition at  $\sim 27^\circ\text{C}$ . A new state of the oil, induced by this transition, is distinguished by a sizeable increase in the mass of deposits at any measurement’s temperature. The thermally transformed oil apparently is in “high temperature equilibrium” (HTE) state above  $27^\circ\text{C}$  and, on cooling, exhibits a remarkable temperature hysteresis of at least  $10^\circ\text{C}$ . Namely, in month-long experiments relaxation from the “quenched” (metastable) HTE state to the LTE state (denoted by filled symbols in Figure 1) was observed only below the above mentioned specific temperature of  $17^\circ\text{C}$  and just in 40% of measurements (cf. the respective bifurcation of data points in Figure 1). At temperatures not lower than  $17^\circ\text{C}$ , the “quenched” HTE state appeared to be practically stable. In original experiments (Figure 1) we never observed relaxation of the oil to the LTE state. Moreover, at  $20^\circ\text{C}$  we again have tested the thermally transformed model oil after six months storage at RT ( $18\text{-}20^\circ\text{C}$ ) and still observed a mass of deposits characteristic for the “quenched” HTE state.

**3.2. Viscosity measurements.** Some of the deposition experiments have been supplemented by measurements of viscosity in the model oil with the same thermal history. The results are presented in

Figure 2. Open and filled symbols denote the same data as in Figure 1. In this case HTE and “quenched HTE” states in oil, subjected to pre-heating above 27°C are distinguished by decreased dynamic viscosity. In viscosity measurements we have never observed relaxation of the oil from a metastable/quenched state (open symbols) to the LTE state (filled symbols), probably due to a comparatively smaller number of experiments.

In a number of publications it has been shown that measurements of a temperature-dependent Arrhenius activation energy of a viscous flow  $E_{act}(T)$  may provide information on types/strengths of intermolecular bonds in asphaltene dispersions.<sup>16,17,21</sup> Hence, a special series of viscosity experiments has been conducted to obtain information on  $E_{act}(T)$  in the LTE and HTE/metastable states of the studied model oil. Namely, in experiment #1 a fresh sample of thermally untreated model oil (stored for a long time at RT) has been cooled to 10°C and its viscosity  $\eta$  has been measured at temperatures, increased by 1°C increment up to 36°C (i.e. above the structural transformation). Afterwards, the sample (presumably transformed to HTE state) again has been subjected to the same cooling-heating cycle in experiment #2. A temperature-dependent Arrhenius activation energy of a viscous flow was determined in sliding temperature intervals  $\Delta T=4-5^{\circ}\text{C}$  by fitting straight lines to the plots of  $\ln(\eta)$  vs. reciprocal measurement temperature  $1/T$ .

The results for  $E_{act}(T)$  are presented in Figure 3. Filled and open symbols denote the data for experiments #1 and #2, respectively. It can be seen that, generally,  $E_{act}$  remains fairly constant in the range of 18-21 kcal/mol, which is close to 14-20 kcal/mol, reported by other authors for asphaltene activation/association energies.<sup>14</sup> The observed LTE→HTE phase transition obviously is endothermic (i.e. first-order<sup>7,12</sup>), as it is accompanied by a transient increase of activation energy, while the observed change of  $E_{act}$  by 10-12 kcal/mol is typical to a cooperative break-up of non-covalent (hydrogen) bonds.<sup>22</sup> Finally, an apparent significance of  $T\approx 17^{\circ}\text{C}$  is again seen in Figure 3.

## 4. Discussion

**4.1 Basic assumptions.** In accordance with our previous results (cf. Introduction), a plausible conclusion is that the observed transformations of the state of the studied multicomponent model oil are governed by equilibrium-metastable transitions in asphaltene colloids. A schematic description may be that at  $\sim 27^{\circ}\text{C}$  a structural transformation occurs in core-corona structures of asphaltene MNCs. This affects interaction potentials and sizes of these basic nanoparticles, as well as of their colloidal aggregates.

Plausible molecular mechanisms may be discussed by employing the approach of W. Loh,<sup>10</sup> who pointed a parallel between the structural/aggregation properties of asphaltenes and of amphiphilic block copolymers. This parallel implies the use of a nomenclature, which may be regarded as unconventional in asphaltene studies and, hence, requires some definitions. E.g., “copolymer” may be defined as “a macromolecule consisting of more than one type of building unit”.<sup>22</sup> For a non-associated molecule a commonly used term is “monomer”. With block copolymers, this term would cause confusion with the macromolecule building units/blocks. Hence, the non-aggregated state of a copolymer/amphiphile is called as “unimer”, while “monomer” is a term for an individual building unit/block.<sup>10</sup> Another difference is related to the implications of the word “micelle”. In normal surfactant solutions, “micelles” would be aggregates that are stable in a significant range of environmental conditions (e.g., concentration, temperature, and presence of additives) as to produce an aggregate with constant aggregation number, size, and shape. For copolymer solutions, whose aggregation process is significantly more complex, the alternative would be using the word “nanoaggregate” (or “molecular nanocluster”, “MNC”), for which a continuously changing assembling entity is expected. Finally, a suspension of evolving (e.g., thermally responsive) copolymer nanoaggregates is commonly referred to as “microgel”.<sup>23</sup>



Two basic building units/blocks of asphaltene “copolymers” are fairly well-known, these are a rigid pericondensed aromatic ring system and a flexible alkane chain.<sup>2,3</sup> A “fluffy” (compressible) character of diblock asphaltene nanoaggregates / MNCs recently has been emphasized by O.C. Mullins,<sup>3</sup> as shown in Figure 4a. In large measure, this structure is in concert with a basic “asphaltene crystallite” of the T. F. Yen’s model introduced many years ago.<sup>1</sup> An important difference is that the nanoaggregate of Figure 4a is not space-filling. The aromatic systems do not form compact face-to-face stacks, expected in case of predominant  $\pi$ - $\pi$  bonding<sup>1-4</sup> but, instead, there are multiple edge-to-face contacts as well as alkane – aromatic interactions, implying a significant contribution of other types of bonds (cf. Section 4.4).

For further discussion it is important that a core-corona structure of this asphaltene nanoparticle is virtually similar to that of a typical thermally responsive microgel nanoparticle (Figure 4b) composed of more conventional diblock copolymers (e.g. with PEO-PPO blocks<sup>24</sup>).

**4.2 Evolution of particle size in asphaltene dispersions.** In support of the above assumptions, let us again consider the viscosity results of Figure 2. It is well known that viscosity of suspensions (at least in a hard sphere approximation) depends only on the volume fraction of the particles. This concept can also be used for particles of variable size; however, the effective volume fraction  $\phi_{eff}$  has to be considered. In dilute solutions, the relative viscosity  $\eta_{rel}$  is related to the effective volume fraction by the Einstein-Batchelor equation:<sup>25</sup>

$$\eta_{rel} = \eta / \eta_s = 1 + 2.5\phi_{eff} + 5.9\phi_{eff}^2 \quad (2)$$

$\eta$  and  $\eta_s$  denote the viscosity of the suspension and the solvent, respectively. Hence, for suspensions of a constant mass concentration (as in Figure 2),  $\eta(T)$  data may be used to evaluate variations of an effective radius of dispersed particles  $R_{eff}$ , as it is directly proportional to  $(\phi_{eff})^{1/3}$ . The

results of such evaluation are shown in Figure 5. Step-like temperature dependence can be seen, indicating an abrupt shrinkage of asphaltene particles after a phase transition at  $\sim 27^{\circ}\text{C}$ .

A decrease of suspension's viscosity in a narrow temperature range (Figure 2) as a result of particle shrinkage (Figure 5) also is typical for thermally responsive microgels, as illustrated in Figure 6 (data from Ref. 27). In the latter systems, particle shrinkage on heating occurs at a specific "lower critical solution temperature" (LCST) via fairly well-known molecular mechanisms. In particular, LCST commonly is an attribute of a first-order phase transition in microgel nanoparticles (nanoaggregates), ascribed to an endothermic break-up of non-covalent (hydrogen) bonds,<sup>26,27</sup> once again in analogy with the observed behavior of  $U_{act}$  in asphaltene dispersions (cf. Section 3.2). A less common, but fairly well-known, property of microgels is a temperature hysteresis of a reverse transition on cooling. Typically, the transition temperature difference is only  $2\text{-}5^{\circ}\text{C}$  where as in some systems it can be large as  $10^{\circ}\text{C}$ ,<sup>28</sup> i.e. equal to that, observed in our deposition experiments (Figure 1).

Over the past several years it has been demonstrated<sup>10,23</sup> that microgel-type dispersions of copolymers exhibit novel phase diagrams that are not been observed in conventional colloids. The main reason is that the volume transition of nanoaggregates at LCST significantly affects the interaction potentials. Schematically, the break-up of intra-aggregate bonds facilitates interactions with surrounding molecules/particles/aggregates. The inter-aggregate interactions are repulsive at temperatures below the LCST, typical for a hard sphere contact potential, while above LCST the potential becomes significantly attractive,<sup>23,29</sup> hence the characteristic aggregation points (e.g., CMC) are usually shifted to lower concentrations. Another consequence is a higher surface/interface activity above LCST, e.g. much better adsorption/ retention of copolymers at solid surfaces.<sup>30</sup> Evidently, asphaltene dispersions also exhibit a change of interaction potentials above  $\sim 27^{\circ}\text{C}$ , as substantiated in the next Section.

**4.3 Other experimental evidence of a thermally responsive nature of asphaltene dispersions.** Literature analysis has revealed some experimental results by other authors in favor of our

basic assumption that the observed specific temperature of  $\approx 27^\circ\text{C}$  is singled out by the processes involving solely asphaltenes and not other constituents of our multicomponent model oil. It should be emphasized that in respective publications the existence of this specific temperature remained unnoticed by the authors.

E.g., the authors of Ref. 31 have measured surface tensions vs. concentrations of pure “Brazilian offshore crude oil” C5I and C7I asphaltenes in toluene at 5, 25 and  $45^\circ\text{C}$ . The authors conclude, that “as expected, surface tensions decreased with increase in temperature at the same asphaltene concentration” but do not plot the respective temperature dependencies. In Figure 7 we show such a plot for asphaltene concentration  $\approx 12.5$  g/L, close to that in our model oil. The temperatures in vicinity of  $\sim 27^\circ\text{C}$  are clearly singled out, indisputably due to some physicochemical processes involving asphaltenes. An abrupt decrease of surface tension at higher temperatures is qualitatively similar to an increase of a surface activity above LCST in copolymer/microgel systems.

In other experiments,<sup>15</sup> thermally-controlled viscosity measurements were employed to identify “CMC” and other “aggregation points” of pure “Arabian medium heavy resid” asphaltenes in 1-methyl naphthalene. Here, again, the specific temperatures were not noticed, but may be easily revealed by more detailed inspection of the presented data. As an example, Figure 8 shows an enlarged part of “CMC” dependence from Figure 10 of Ref. 15 (filled symbols connected with a dashed line). An accelerated decrease of “CMC” close to  $27^\circ\text{C}$  is clearly seen and may be further emphasized by plotting a derivative of the temperature dependence (solid line). As noted above, lower “CMC” values may be regarded as indicative of increased interaction potentials in asphaltene dispersions above an apparent LCST of  $\approx 27^\circ\text{C}$ .

In relation to our deposition experiments (Figure 1), increased interaction activity of asphaltenes may be responsible (at least partially) for the observed increase in the mass of deposits from the oil in

HTE and metastable states. Another reason for increased deposition may be the observed viscosity decrease (Figure 2), which should facilitate a transport of depositing material to a metal surface.

**4.4 Apparent importance of intra-aggregate hydrogen bonding.** The means by which asphaltenes interact to form nanoaggregates in petroleum remains the subject of speculation but noncovalent association by formation of charge-transfer  $\pi$ - $\pi$  complexes, hydrogen bonds and by van der Waals attraction have been cited as causative mechanisms.<sup>1-3,32</sup> The discussed similarities with LCST microgels implies that the relative role of H-bonding in asphaltene dispersions may be underestimated. Indeed, LCST normally is observed in copolymers whose aggregation/solubility is *controlled by the strength of hydrogen bonding*.<sup>23,25,33</sup> The origin of the phase transition at LCST is mainly associated with the reorganization/destruction of the hydrogen bonding at higher temperatures, resulting in a first-order transition to compact nanoaggregates. A characteristic abruptness of the transition (consider Figures 1,2) in microgels is due to a highly cooperative character of a break-up of multiple H-bonds. Moreover, the strength of hydrogen bonding is a determining factor in the values of LCST, which for a wide range of microgel systems (as well for the studied asphaltene dispersions) are in a moderate interval of “physiological temperatures”:  $\sim 25 - 40^\circ\text{C}$ .

Some specific features of hydrogen bonding also may be responsible for the presumed “fluffiness” of asphaltene nanoaggregates (cf. Figure 4a). Namely, by virtue of possessing large fused aromatic-ring systems, asphaltene molecules could have been expected to associate via  $\pi$ - $\pi$  interactions into compact face-to-face stacks<sup>1-3</sup> (as illustrated in Figure 9a for the simplest system of a benzene dimer). Hydrogen bonds, in general, are not much stronger than  $\pi$ - $\pi$  forces, but their directive power is more pronounced, hence the space-filling stacks may be distorted, as shown in Figure 9b. In this directional bonding there is a significant interaction between a hydrogen bond donor (like the  $>\text{C-H}$  group) and the centre of an aromatic ring, which acts as a hydrogen bond acceptor. The role of H-bonding to aromatic systems was not appreciated until after such bonds had been observed in protein-

drug complexes.<sup>34</sup> More recently, it has been shown that the discussed edge-to-face C-H/ $\pi$  interactions are somewhat weaker than classical H-bonding and the preferred geometry is T- or L-shaped.<sup>35</sup>

Finally, in relation to hydrogen bonding, we have to address an issue of trace water in asphaltene dispersions. In some comparatively recent publications it has been stated that the presence of trace water (of water-asphaltene H-bonding) is “the driving force” of the measurable asphaltene aggregation phenomena<sup>36,37</sup> hence, presumably, all previously reported experimental data should be reconsidered. In this respect, we strongly support the opinion of the authors of Ref. 3, which is as follows. We have not determined the effect of trace water on asphaltene nanoaggregates here, nor have we tried to exclude trace water from our measurements. It would not be surprising to find that water might of some importance. Natural crude oil systems have trace water; therefore, the results contained herein are likely related to crude oils in the natural state. Furthermore, the results herein are directly related to results from almost all results reported to date on nanoaggregates (or on aggregation stages) in asphaltenes, because other laboratories also do not remove trace water in their asphaltene experiments.

Moreover, a quantitative inspection of the original experimental results on water in asphaltene/toluene solutions<sup>37</sup> shows that the qualitative “driving force” statement is, at least, over-exaggerated. Namely, in Ref. 37, “Figure 1 shows the solubility of water as a function of asphaltene concentration in toluene for several asphaltenes”. At asphaltene concentration of 15 mg/L (close to that in our experiments) the measured absolute water uptakes are typically in the range from  $\sim 0.047$  to  $\sim 0.064$  g/kg toluene (with  $\sim 0.077$  g/kg toluene for one sample), while in pure dried solvent water solubility is  $\sim 0.046$  g/kg toluene. Hence, the net w/w ratio of water solubilized by asphaltenes is from  $\sim 0.00004$  to  $\sim 0.001$  (with a single maximum value of  $\sim 0.0018$ ). Assuming for MW of asphaltenes a typical value<sup>2,3,37</sup> of 750 Dalton, the respective molar ratios are from  $\sim 0.002$  to  $\sim 0.04$  (maximum of  $\sim 0.07$ ). Hence, from the discussed experimental results it follows that only from 0.2% to 4% (maximum

7%) asphaltene molecules make bonds with water. This amount is clearly too low to make H-bonding with water a prominent factor (let alone “the driving force”) in formation of the basic asphaltene nanoaggregates.

## 5. Conclusions

Measurements of various properties of asphaltene-containing fluids indicate the existence of a first order phase transition (PT) in asphaltene colloids at  $\sim 27^{\circ}\text{C}$ . The transformed structures may be quenched to long-lived (up to six months) metastable states at lower temperatures. By a number of qualitative and quantitative attributes PT of asphaltenes resembles volume phase transitions, controlled by the properties of hydrogen bonding, in thermally responsive microgel dispersions of block copolymers. Moreover, the known structures of asphaltene and copolymer nanoparticles appear to be virtually similar. In particular, a discussion of asphaltene – microgel resemblance indicates that the thermally responsive “fluffy” structure of asphaltene nanoaggregates may be controlled by specific edge-to-face hydrogen bonds to aromatic systems.

## Figure captions

**Figure 1.** Effects of deposition temperature and of the thermal history of asphaltene-rich model oil on the mass of deposits at steel samples. Filled symbols – data for the “room temperature equilibrium” oil, never heated above 27°C. Open symbols - data for the oil at least once pre-heated to 28°C, or to higher temperatures (note bifurcation/bistability of low-temperature deposits in this data set).

**Figure 2.** Effects of deposition temperature and of the thermal history of asphaltene-rich model oil on its dynamic viscosity. Filled symbols – data for the oil never heated above 27°C. Open symbols - data for the oil at least once pre-heated to 28°C, or to higher temperatures.

**Figure 3.** Activation energies of viscous flow obtained: 1) by first-time heating from 10°C to 36°C of an oil sample in “room temperature equilibrium” state (filled symbols); 2) in a repeat experiment with the same sample.

**Figure 4.** Schematic structures of: a) a “fluffy” asphaltene molecular nanocluster, introduced by O. C. Mullins<sup>3</sup> ; b) a typical thermally responsive microgel nanoparticle, composed of diblock copolymers.<sup>24</sup>

**Figure 5.** Estimated variations of an effective radius of dispersed asphaltene particles in viscosity experiments of Figure 2.

**Figure 6.** Normalized variations of an effective radius of dispersed microgel particles in a vicinity of the lower critical solution temperature (viscosity experiments of Ref. 27).

**Figure 7.** Surface tensions vs. temperature for toluene solutions of C5I (open symbols) and C7I (filled symbols) asphaltenes. Adapted from Ref. 30.

**Figure 8.** Non-monotonous temperature dependence of “CMC” for asphaltenes in in 1-methyl naphthalene (experimental points, connected by a dashed line - adapted from Ref. 15) and its first derivative (solid line).

**Figure 9.** Compact  $\pi$ - $\pi$  stacking of aromatic systems (a) and a distortion of this space-filling configuration as a result of hydrogen bonding (b).

## References

(1) Sheu, E. Y.; Mullins, O. C., Eds. *Asphaltenes: Fundamentals and Applications*; Plenum Press: New York, 1995.

(2) Andreatta, G.; Bostrom, N.; Mullins, O. C. High- $Q$  Ultrasonic Determination of the Critical Nanoaggregate Concentration of Asphaltenes and the Critical Micelle Concentration of Standard Surfactants. *Langmuir* **2005**, *21*, 2728-2736.

(3) Andreatta, G.; Goncalves, C. C.; Buffin, G.; Bostrom, N.; Quintella, C. M.; Arteaga-Larios, F.; Perez, E.; Mullins, O. C. Nanoaggregates and Structure-Function Relations in Asphaltenes. *Energy Fuels* **2005**, ASAP Article 10.1021/ef0497762 S0887-0624(04)09776-2.

(4) Evdokimov, I. N.; Eliseev N. Yu.; Akhmetov, B. R. Assembly of Asphaltene Molecular Aggregates as Studied by near-UV/visible Spectroscopy.; I. Structure of the Absorbance Spectrum. *J. Petr. Sci. Eng.* **2003**, *37*(3-4), 135-143; II. Concentration Dependencies of Absorptivities. *J. Petr. Sci. Eng.* **2003**, *37*(3-4), 145-152.

(5) Evdokimov, I. N.; Eliseev N. Yu.; Akhmetov, B. R. Initial Stages of Asphaltene Aggregation in Dilute Crude Oil Solutions: Studies of Viscosity and NMR Relaxation. *Fuel* **2003**, *82*(7), 817-823.



- (6) Sheu, E. Y. Petroleum Asphaltene-Properties, Characterization, and Issues. *Energy Fuels* **2002**, *16*(1), 74-82.
- (7) Akhmetov, B. R.; Evdokimov, I. N.; Eliseev, N.Yu. Some Features of the Supramolecular Structures in Petroleum Media. *Chemistry and Technology of Fuels and Oils* **2002**, *38*(4), 266-270.
- (8) Evdokimov, I. N.; Eliseev N. Yu.; Akhmetov, B. R. Asphaltene Dispersions in Dilute Oil Solutions. *Fuel* (submitted)
- (9) Evdokimov, I. N. A Transition From Monomeric To Associated Asphaltenes in Crude Oil Solutions. 2nd Mercosur Congress on Chemical Engineering and the 4th Mercosur Congress on Process Systems Engineering (ENPROMER 2005). Village Rio das Pedras, Club Med, Rio de Janeiro, Brazil, 2005.
- (10) Loh, W. Block Copolymer Micelles. In *Encyclopedia of Colloid and Surface Science*; Hubbard, A., Ed.; Marcel Dekker: New York, 2002; pp. 802-813.
- (11) Evdokimov, I. N.; Eliseev, N. Yu.; Ulantsev, A. D. Colloid Nanosystems in Petroleum Media. *Nauka i Tehnologija Uglevodorodov* **2001**, *1*, 55–59 (In Russian).
- (12) Evdokimov, I. N.; Eliseev, N. Yu.; Eliseev, D. Yu. Rheological Evidence of Structural Phase Transitions in Asphaltene-Containing Petroleum Fluids. *J. Petr. Sci. Eng.* **2001**, *30*(3/4):199-211.
- (13) Sirota, E. B. Understanding the Physical Structure of Asphaltenes. Abstr. of 5<sup>th</sup> Int. Conf. on Petr. Phase Behavior and Fouling, Banff, Alberta Canada, 2004.
- (14) Wong, G. K.; Yen, T. F. An Electron Spin Resonance Probe Method for the Understanding of Petroleum Asphaltene Macrostructure. *J. Petr. Sci. Eng.* **2000**, *28*, 55–64.

- (15) Priyanto, S.; Mansoori, G. A.; Suwono, A. Measurement of Property Relationships of Nano-Structure Micelles and Coacervates of Asphaltene in a Pure Solvent. *Chem. Eng. Sci.* **2001**, *56*, 6933–6939.
- (16) Evdokimov, I. N.; Eliseev, N. Yu.; Eliseev, D. Yu. Thermophysical Properties and Phase-Behaviour of Asphaltene-Containing Petroleum Fluids. *Fluid Phase Equilibria* **2003**, *212*(1/2), 269-278.
- (17) Evdokimov, I. N.; Eliseev, N. Yu.; Eliseev, D. Yu. Effect of Asphaltenes on the Thermal Properties of Emulsions Encountered in Oil Recovery Operations. *Fuel* **2004**, *83*(7/8), 897-903.
- (18) Evdokimov, I. N. Well-Defined Metastable (Transient) States of Asphaltene Colloids. The 2004 International Conference on Heavy Organic Depositions (HOD 2004), Los Cabos, Baja, Mexico, November 2004.
- (19) Adamson, A. W. *Physical Chemistry of Surfaces.*; 3d Edition; John Wiley & Sons: New York, 1976.
- (20) Taylor, S. E. The Electrodeposition of Asphaltenes and Implications for Asphaltene Structure and Stability in Crude and Residual Oils. *Fuel* **1998**, *77*(8), 821-828.
- (21) Miura, K.; Mae, K.; Hasegawa, I.; Chen, H.; Kumano, A.; Tamura, K. Estimation of Hydrogen Bond Distributions Formed between Coal and Polar Solvents Using in Situ IR Technique. *Energy Fuels* **2002**, *16*(1), 23-31.
- (22) Seymour, R. B.; Carraher, C. E. *Polymer Chemistry.*; 3rd Ed.; Marcel Dekker: New York, 1992.
- (23) Wu, J.; Hu, Z. Microgel Dispersions: Colloidal Forces and Phase Behavior. In *Dekker Encyclopedia of Nanoscience and Nanotechnology.*; Marcel Dekker, Inc.: New York, 2004; pp. 1967-1976.

- (24) Guenet, J. M. *Thermoreversible Gelation of Polymers and Biopolymers.*; Academic Press: New York, 1992.
- (25) Batchelor, G. K. The Effect of Brownian Motion on the Bulk Stress in a Suspension of Spherical Particles. *J. Fluid Mech.* **1977**, *83*, 97-117.
- (26) Senff, H.; Richtering, W. Temperature Sensitive Microgel Suspensions: Colloidal Phase Behavior and Rheology of Soft Spheres. *J. Chem. Phys.* **1999**, *111*(4), 1705-1711.
- (27) Bigi, A.; Cojazzi, G.; Panzavolta, S.; Roveri, N.; Rubini, K. Mechanical and Thermal Properties of Gelatin Films at Different Degrees of Glutaraldehyde Crosslinking. *Biomaterials* **2001**, *22*, 763–768.
- (28) Sekimoto, K. Temperature Hysteresis and Morphology of Volume Phase Transition of Gels. *Phys. Rev. Lett.* **1993**, *70*(26), 4154-4157.
- (29) Arleth, L.; Xia, X.; Hjelm, R. P.; Wu, J.; Hu, Z. Volume Transition and Internal Structures of Small Poly(*N*-isopropylacrylamide) Microgels. *J. Polymer Sci. B: Polymer Physics* **2005**, *43*, 849–860.
- (30) Miura, M.; Cole, C. A.; Monji, N.; Hoffman, A. S. Temperature-Dependent Absorption/Desorption Behavior of Lower Critical Solution Temperature (LCST) Polymers on Various Substrates. *J. Biomater. Sci. Polym. Ed.* **1994**, *5*(6), 555-568.
- (31) Ramos, A. C. S.; Haraguchi L.; Notrispe, F. R.; Loh, W.; Mohamed, R. S. Interfacial and Colloidal Behavior of Asphaltenes Obtained from Brazilian Crude Oils. *J. Petr. Sci. Eng.* **2001**, *32*(2-4), 201-216.
- (32) Speight, J. G. The Chemical and Physical Structure of Petroleum: Effects on Recovery Operations. *J. Petr. Sci. Eng.* **1999**, *22*(1-3), 3-15.

(33) Dai, S.; Tam, K. C. Isothermal Titration Calorimetric Studies on the Temperature Dependence of Binding Interactions between Poly(propylene glycol)s and Sodium Dodecyl Sulfate. *Langmuir* **2004**, *20*(6), 2177-2183.

(34) Levitt, M.; Perutz, M. F. Aromatic Rings Act as Hydrogen Bond Acceptors. *J. Mol. Biol.* **1988**, *201*, 751-754.

(35) Jennings, W. B.; Farrell, B.M.; Malone, J. F. Attractive Intramolecular Edge-to-Face Aromatic Interactions in Flexible Organic Molecules. *Acc. Chem. Res.* **2001**, *34*(11), 885-894.

(36) Andersen, S. I.; del Rio, J. M.; Khvostitchenko, D.; Shakir, S.; Lira-Galeana, C. Interaction and Solubilization of Water by Petroleum Asphaltenes in Organic Solution. *Langmuir* **2001**, *17*(2), 307-313.

(37) Khvostichenko, D. S.; Victorov, A.I.; Andersen, S. I. Trace Water-Asphaltene Interaction in Organic Solvents. Proceedings of the 2002 International Conference on Heavy Organic Depositions (HOD-2002), Puerto Vallarta, Jalisco, Mexico, November 17-21, 2002. CD-Rom Edition.

Figures

Figure 1.

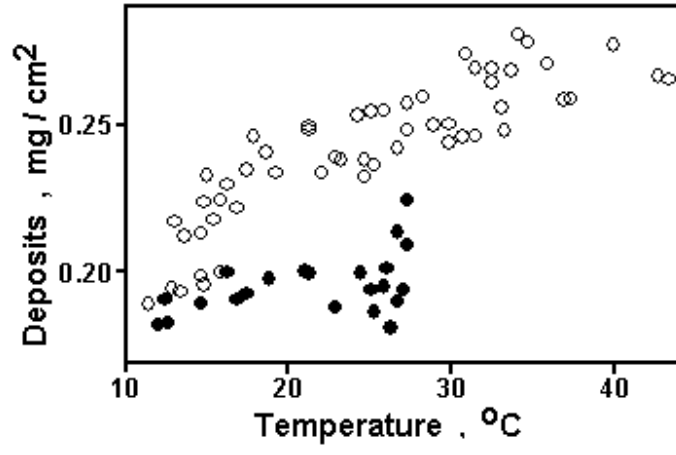


Figure 2.

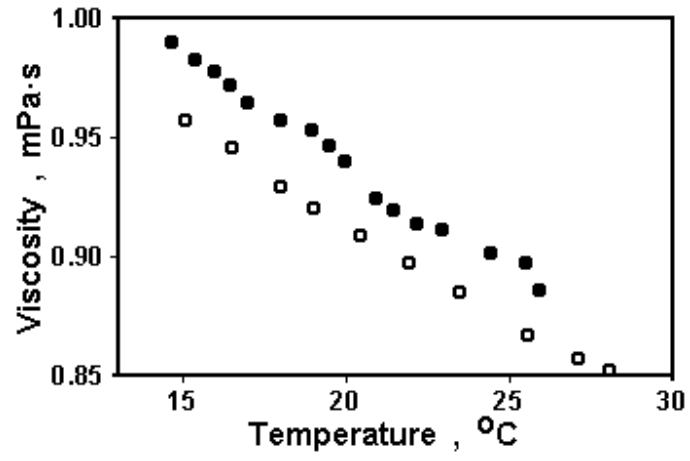


Figure 3.

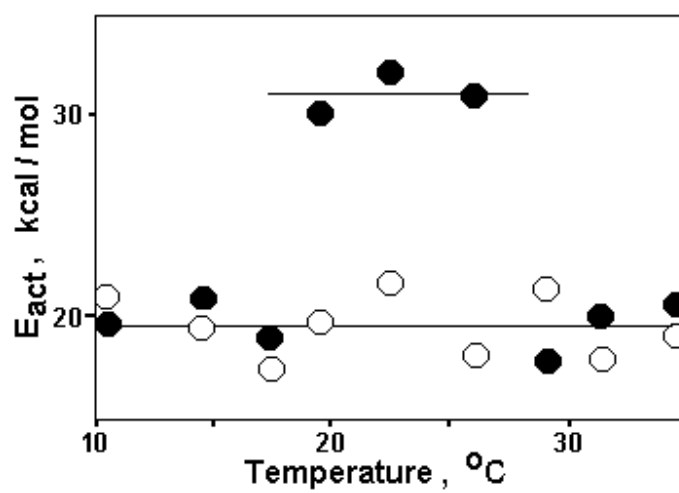


Figure 4.

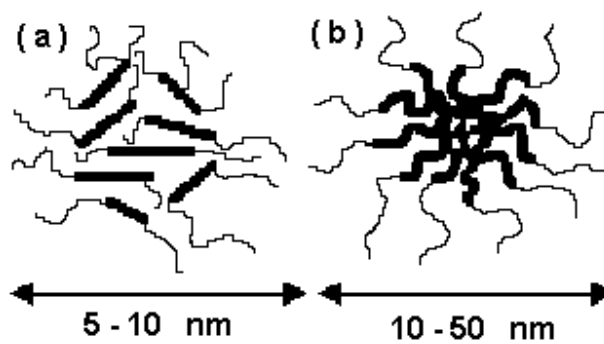


Figure 5.

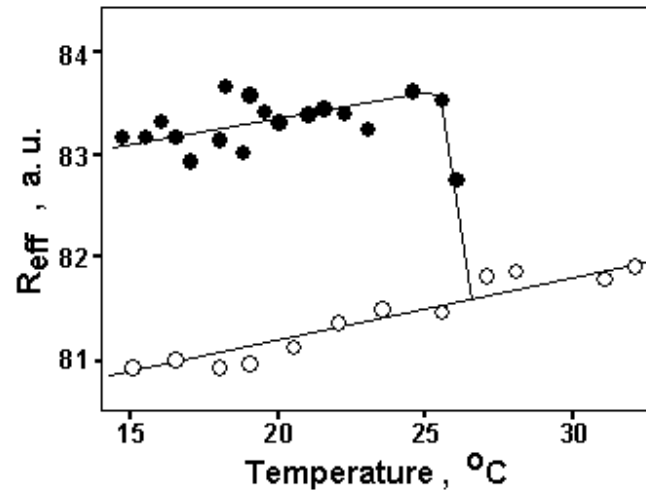


Figure 6.

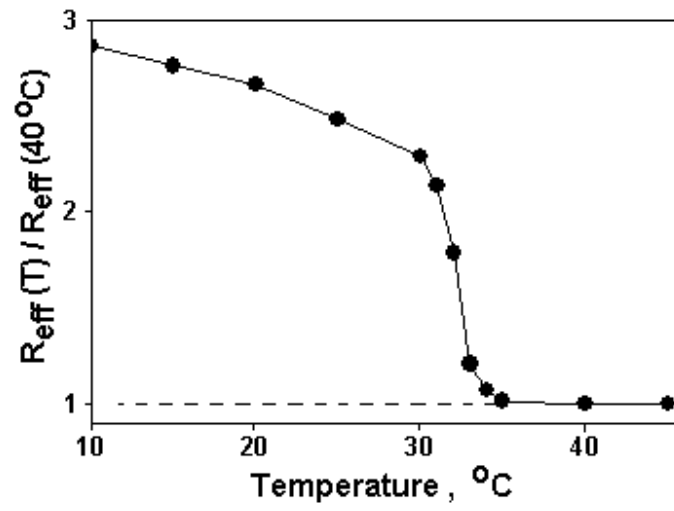


Figure 7.

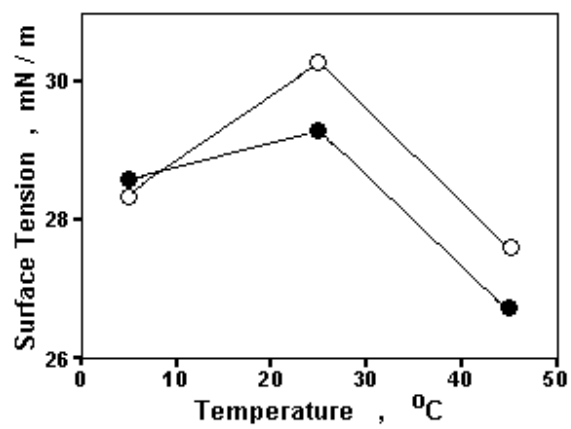


Figure 8.

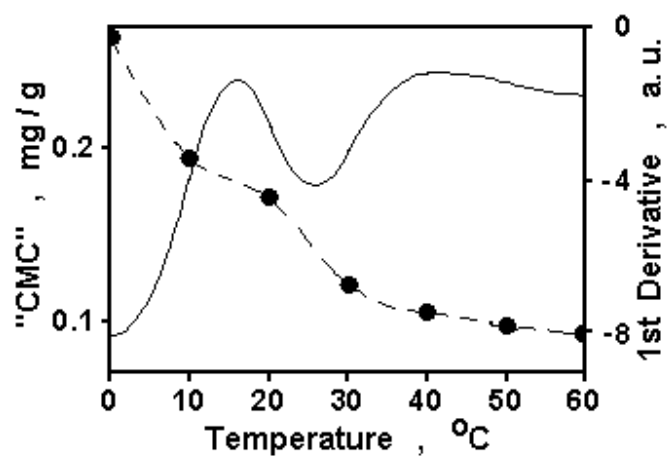




Figure 9.

